

## Fatigue in gas turbine components

A. K. RAY, B. GOSWAMI<sup>1</sup>, S. B. KUMAR<sup>2</sup> and S. K. SAHAY<sup>3</sup>

National Metallurgical Laboratory, Jamshedpur-831007

<sup>1</sup>R.V.S. College of Engineering and Technology, Jamshedpur - 831 012

<sup>2</sup>National Institute of Foundry and Forge Technology, Hatia, Ranchi-834 003

<sup>3</sup>National Institute of Technology, Jamshedpur-831014

**Abstract :** Life of hot section components of gas turbine performs at the limiting condition of exposure when thermal barrier coating (TBC) is applied. Insulation and resistance to high temperature corrosion rise efficiency of engines. TBC is applied in various forms in different sectors, which included thick TBC, thin TBC, and duplex/triples/multilayered coatings of ceramics and metal compositions. Bond coat (BC) and topcoat (TC) composition and treatment processes are exploited for optimum failure free design. However combined HCF-LCF performances at high temperature reduce life. Mismatch reversal of relative stresses often has been used to be variable for optimization. In cases of prolonged trouble free exposure in service, the atmospheric contaminant appears to be damaging. These include wear of grit and dust, attack of reaction products of fuel, and formation of SiO<sub>2</sub>-FexOy composed ceramic sinters in place of ceramic insulation coatings. Fatigue is reviewed in this paper to study characteristics of materials of various turbine components at high temperature. Effects of temperature of exposure in different instances are to produce damage mechanisms and requirement of different preventive attention.

**Keywords :** Fatigue, Strain range partitioning, Thermomechanical fatigue (TMF), Fatigue crack propagation (FCP), High cycle fatigue (HCF), Life prediction, Thermal barrier coating (TBC), Topological close packed structure (TCP), Superalloy, High rate fully reversed strain cycle, Combustion chamber.

### INTRODUCTION

In this review both the TBC coated and uncoated component properties are studied. The aim is to assess the mode of progress to understand the most probable failure consequences. Experimental compromises have showed various extents of improvements on aeroengines, e.g. DART, SPEY250 and RB211. Where corrosion from salt contamination or otherwise is rectified by aluminisation of metallic components and subsequent YSZ deposition.

Thermal barrier coatings are prepared by different spray technique. Previously surface hardening of similar events has been done by cementation process and on metallic material based. The present states of surface preparation emphasize on porous deposit of ceramics on a roughened as sprayed metallic bonding layer surface on substrate. Plasma spray is one of such process, where different torch design and industrially feasible form of variable control makes the process versatile to apply this coating at any position, shape and cleanliness. Fatigue failure in gas turbine components that operated at high temperature is often found as a point of interest. Various simulations are applied to study the different types of fatigue like load controlled high cycle fatigue (HCF), strain controlled low cycle fatigue test (LCF) and their combinations, creep-fatigue, corrosion fatigue and thermo-mechanical fatigue under different temperature ranges and isothermal state, where time factor is considered for compensating environmental effects. Designing of failure free approaches and respective life prediction mostly appears to

---

\* Corresponding Author Email : asokroy@nmlindia.org

be based on empirical formulations. Moreover innovations appears to be fracture mechanics based experiments. Since the lightweight philosophy is adopted in every design so most of study is done on small crack only, because of thinner section of components. Combination of HCF-LCF and creep-fatigue-oxidation of components under high vibratory stresses and associated temperature has often found to be the mode of failure in actual cases.

Correct assessment of variables and their introduction to empiricism widens the technique to expose the deficient area. On the other hand adoption of stabilizer modification may improve performance from the front of fundamentalism. For example YSZ to CYSZ (ceria yttria stabilized zirconia) or SYSZ (scandia yttria stabilized zirconia) open new avenues in an industrial scale. Discrete senses of exploratory information are summated in this paper to produce a generalized sense about nature of exploitation of variables to technically update the probability of improvement. For example introduction of variables (in response to liner of combustor in a gas turbine) of reaction quench, flame turbulence, combustion oscillation from the front of environmental consideration appears to be deficits to empiricism. However the fundamentalist approaches of nickel diffusion to the bond coat (BC)-topcoat (TC) interfaces to form spinal structure is a limitation to the existing system under any consideration, when life is concerned.

Coating failure of hot section components in aero-engine sector, mostly appear after landing and upon cooling down of engine instead of take off load bearing schedule and respective optimum engine performance. Consideration of a composite equation consisting of variables that relates HCF-LCF-creep-oxidation/corrosion phenomenon that plays over the every possible incident to coating/substrate failure appears to be deficient in the simulation. The experiments mostly have carried over a philosophy that occupies an intermediate position within empiricism and requirement, where failure free or infinite life design is the desire to obtain before industrial feasibility.

### **HIGH CYCLE FATIGUE**

Aircraft gas turbine engines demand durability, high reliability, lightweight, and high performance. The Goodman Diagram and Miners rule is used for the aircraft engine design for ensuring safety of critical structural components. It is based on the lifetime failure free design criteria. This design process usually consists of a structural dynamics analysis to determine natural frequencies and mode shapes at certain operating speed ranges and a stress analysis to calculate the dynamic stress distribution for identifying the maximum vibratory stress location or area under a series of given excitation. Once the maximum stresses for each vibration mode are determined, high cycle fatigue assessment is achieved by measuring the margin between the maximum vibratory stress and the material fatigue capability. That is a straight line called Goodman line drawn between the mean ultimate strength at zero vibratory stress and mean fatigue strength at 10<sup>7</sup> cycles (or infinite life). These design criteria, design guides, or design codes are established using the results of a simple deterministic analysis procedure without taking into account the information such as degradation of material properties, scatter in testing data, design experiences, and uncertainties inherent in the operating conditions in the real world. A number of structural failures have occurred in aircraft engines during development, testing, and operational service. These incidents triggers an awareness related to the life time failure free design criteria of the current aircraft engine critical structural components. Turbomachinery blade failures of aircraft engine result from high vibratory stress resulting from the excessive vibration during forced response. Forced response usually occurs under a

non-uniform flow field-operating environment, when the excitation frequency from an unsteady aerodynamic load coincides with any blades material frequency. Hence for an adequate blade design all the resonant conditions could be avoided. Realistically, this is impossible due to the lack of insufficient real world loading information at the time of the analysis and design. In addition, a non-uniform flow field-operating environment creates widely distributed high vibratory stresses resulting in high cycle fatigue (HCF) degradation of metallic structures. In its early stages the accumulating degradation is often very difficult to detect. Furthermore, variability in geometry, aerodynamics, and materials make it difficult to assess vibration cycling with certainty. The effects of the randomness can not be quantified accurately by any traditional deterministic analysis approach. Hence it is beyond the capacity of any approaches to provide the important information regarding risk of failure, or the sensitivities of the design variables to risk. So an innovative probability based reliability HCF design and life prediction methodology for gas turbine engine blades are accounted for variability in geometry and aerodynamic loading, and to calculate important design and maintenance information of sensitivity, (High cycle) fatigue reliability, and associated risk. Y.Sawarin et.al. state that the concept of structural design and operation under technical state conditions for creep or high cycle fatigue is based on the description of deformation process, the analysis of failure associated with creep rupture, high cycle fatigue, crack initiation, and propagation, the establishment of appropriate design criteria and control, and identification of structural responses<sup>[1]</sup>. A.Shyam et.al. have observed another failure incidence that is high cycle fatigue (HCF) in military aircraft gas turbines. The high empirical approach based on Goodman diagram to such a pervasive problem, which is currently employed to estimate HCF capability. However, a fracture mechanics, threshold based HCF approach is highly desirable. Mechanisms of crack arrest associated with fatigue crack propagation (FCP) thresholds are complex in nature and there is a large discrepancy between results predicted from theoretical threshold models and experimentally determined values. These models deal exclusively with either intrinsic or extrinsic factors affecting the threshold without taking into account their synergistic interactions. To address these problems, data under engine HCF conditions is necessary. Elevated temperature long crack FCP tests have been performed at high frequencies in a nickel base turbine disk alloy under a variety of experimental conditions. Four important factors affecting threshold (temperature, frequency, microstructure, and load ratio) have been systematically varied in order to understand the relative importance of individual factors and the level of interaction between them<sup>[2]</sup>. Fatigue crack propagation (FCP) tests have been also conducted on powder metallurgy nickel-base superalloys KM4 at temperatures of 293, 823, and 923K. Different heat treatments are investigated, one yielding a relatively coarse grain size and another yielding a fine grain size. Tests are conducted at 100Hz and 1000Hz and at load ratios between 0.3 and 0.7. In the Paris regime trends observed at high frequencies for KM4 are identical to those observed by earlier investigations at lower frequencies. Coarse grains, low load ratios, low temperatures, and higher frequencies generally results in lower crack propagation rates. However in contrast to Paris regime behavior, thresholds are a complicated function of microstructure, load ratio, temperature, and frequency, and the only variable in a consistent trend in threshold is the load ratio. For example threshold increases from 100 to 1000Hz for the fine-grained materials at 823K, but decreases with the same frequency vibration at 923K. One reason for this complexity is a change to inter-granular fracture in the fine-grained microstructure at 923K. This is beneficial for high frequency thresholds. Higher load ratios and lower frequencies promote inter-granular fracture. However, not all of the complexity can be explained by fracture mechanisms. Scanning electron microscope (SEM) stereo-fractography is utilized to determine

quantitative measures of fracture surface roughness. The most quantitative measure is found to be standard deviation of fracture surface height, which is a physically meaningful length parameter and which correspond to about half the grain size during room-temperature fatigue at near threshold DK levels. The roughness of the fracture surface is found to increase as the load ratio is increased for both microstructures. For the coarse grained microstructure, there is a direct correlation between fracture toughness and FCP threshold over the entire range of temperature, frequencies, and load ratios. However, measurements of closure loads indicate that roughness induced closure is not the sole reason for the varying FCP thresholds<sup>[2]</sup>.

Fracture characteristics and fracture mechanisms in a nickel base single crystal superalloy have been studied by J.H.Zhang et.al. The composition of superalloy is Ni-15.6Cr-8.4Co-0.74W-3.8Al-3.82Ti-1.16Ta. Heat-treated specimens are subjected to high cycle fatigue under load control at 1073K and 85Hz. The high cycle fatigue strength obtained from the S-N curve is 538 Mpa, which is greater than the same reported for the alloys IN738, and DS38G. SEM fractographs show cleavage and tearing dimple modes of fracture. These further indicate that the fracture modes are associated with planer slip, dislocation cell formation, and formation of low angle grain boundaries. TEM images reveal that  $\gamma$ -morphology changed from cubical to spherical during high cycle fatigue<sup>[3, 4]</sup>. Examination has been made on ratio of static mean stress to HCF stress amplitude and influence of notches on long term HCF endurance. HCF data is correlated with creep rupture data by a combination of the method of Keil and Maier and of the Moore-Kommers-Jasper diagram. Possibility of interpolation replaces costly long term HCF tests in creep range by short term tests at high temperature superposition of HCF and LCF loading leads to life time reductions. This is explained by simple drainage accumulation rules for small HCF stress amplitudes<sup>[5]</sup>. The results stated by B.Gieseke and V.K.Sikka of high cycle fatigue tests at 923K on several cast Ni3Al alloys are reported and compared with cast IN-731C. These alloys include IC-221M and several variations to the IC-221M composition. The effect of casting temperature is investigated using castings poured at three different temperatures spanning a 329K range. The results show that IC-221M cast at the highest temperature has the best fatigue strength, exceeding that for IN-713C. In these alloys, crack initiation occurs at shrinkage microporosity and the effect of casting temperature on porosity is related to the observed differences in fatigue lives<sup>[6]</sup>.

### CREEP FATIGUE

Considerable effort has been made to understand of crack growth behavior under fatigue loading at elevated temperatures, where creep, fatigue and oxidation may contribute to failure concurrently. Depending on the specific materials and loading conditions, the role of each damage component changes significantly ranging from creep-fatigue in creep-ductile for power plant equipment, oxidation-fatigue in creep-brittle high strength alloys for aerospace applications, and creep-fatigue-oxidation in materials under complex loading conditions such as thermomechanical fatigue. Despite the availability of the large volume of mechanical test results, information pertaining to fracture mechanisms and their relevance to the interaction of creep-fatigue-oxidation remains scarce. To date, there is no unified approach with which the problem of fatigue crack growth at high temperature can be solved in a general manner (J.Tong et.al.)<sup>[7]</sup>. Nickel base superalloys are creep-brittle materials because of their superior tensile strength and low creep ductility. Coffin produce the first significant evidence to suggest that oxidation is primarily responsible for high temperature low cycle fatigue (HTLCF) damage in such materials. Since then the subject has been studied

extensively, dealing with aspects of the subject such as the effects of loading variables and environment. Most of the published work is concerned with established wrought alloys such as Inconel 718 or Waspalloy whilst the performance of the new generation of superalloys developed using powder metallurgy technique requires critical assessment. The new alloys are optimized for high strength but often at the expense of damage tolerance. Research is therefore essential to examine the crack growth behavior in these new superalloys under typical operational conditions, and to establish the relevant damage mechanisms, which may include the combination of creep, fatigue, and oxidation. Experimental and theoretical investigations on the influence of temperature, strain dwells, and crystal orientations on high temperature fatigue-creep behavior of single crystal SRR-99 nickel base superalloy have been performed by S.X.Li and D.J.Smith. For a given temperature and loading condition, the longest fatigue life is observed for tests with [001] orientations, while the [111] orientation yielded the shortest fatigue life. A simple approach is applied successfully to correlate the influence of orientation. Using the function, the shortest fatigue life is observed for tests with a compressive dwell at 1023K, but at 1323K tests with a tensile dwell exhibit the shortest life, compared with continuous cycling tests. Tests with tensile dwells show remarkably longer lives at 1023K, significantly shorter lives at 1323K, and almost identical lives at 1223K; tests with compressive dwells always exhibit shorter lives than continuous cycling tests at all temperatures. The influence of strain dwells on the life of SRR 99 is via the simultaneous effects of mean stress, additional inelastic strain, and time dependent damage. A mean stress modify strain range partitioning method is proposed and used to predict the fatigue creep life<sup>[8, 9]</sup>. The growth rate of fatigue cracks on two single crystal nickel base superalloys, CMSX-6 and SRR-99 along the <001> planes has been rationalized in terms of two interacting crack propagating mechanisms by J.M.Martinez Esnaola et.al.. One attribute to crack tip plastic blunting and the other attributes to the brittle failure of the oxide scales. The role of the oxide scale is two folds as it also wages the crack and modifies the blunting term through a crack closure effect. On the other hand, a positive effective stress intensity range is required to fracture the oxide scale. Fatigue tests are carried out at different temperatures (773-1323K), frequencies (0.001-20 Hz), cycle wave forms and load ratios (0-0.9), with starter crack length of ~100mm. The model predictions match the crack growth rates obtained for both materials. Even though both materials are nickel base superalloys, they have very different oxidation behaviors. CMSX-6 has an improved oxidation resistance over SRR 99. The better life expectancy depends on the applied test temperature and loading cycle<sup>[10]</sup>. Oxidation of single crystal nickel base superalloys influences the fatigue and creep behavior. The absences of grain boundaries in single crystal superalloys (SRR 99) are examined by D.J.Smith et.al. at 1223K to study mechanical behavior in different orientations. It is observed that both the cyclic stress strain response and fatigue life exhibit orientation dependence. This dependence is related primarily to the anisotropy based on the elastic properties of the single crystal superalloy. The elastic modulus of the [111] orientation is larger compared with e.g.[001]. Consequently for tests at the same total strain range [111] specimen exhibits a higher stress range and also a high elastic strain range, thereby leading to shorter fatigue lives. Orientation dependence of mechanical behavior is described in terms of an orientation function<sup>[11]</sup>. An experimental study of M.Matsubara et.al. on the effect of environment on creep-fatigue strength of a single crystal nickel base superalloy CMSX2 reveals that the creep fatigue decreases, as corrosion environment becomes severer. The creep-fatigue lives under PP and CC strain waveform conditions seem to be more sensitive to environment than those under PC and CP conditions<sup>[12]</sup>.

**THERMO-MECHANICAL FATIGUE**

An accurate description of inelastic behavior is a prerequisite for assessing the durability of any structural components. It is especially critical in land based gas turbines where components, such as blades and vanes, are subjected to transient operations during startup and shutdown in addition to periods of steady state operation at high temperature. To simulate the stress-strain responses of critical elements of these components, constitutive equations are required. In a first approximation, they can be used in the uniaxial form to simulate the centrifugal forces and thermal stresses arising from temperature gradient during service. The data of stresses and strains during the entire loading history have to be implemented into a finite element code for successful constitutive models so as to reproduce a wide range of features, such as the Buschinger effect, cyclic hardening or softening, strain rate effect, transient and steady state creep, mean stress relaxation, etc. Drucker stated that the behavior of metals and alloys in the plastic range is enormously essentially infinitely complex. No mathematical expressions no matter how elaborate, can portray the response completely and accurately. However, some formulations can provide reasonable descriptions of material behavior under specific loading conditions. Uniaxial and multiaxial fatigue behaviors under a broader spectrum of mechanical and thermal histories continue to be a topic of concentrated research. However, the effort to create sophisticated formulations might limit practical usage if the implementation of the algorithmic into finite element code becomes time consuming. Owing to the complexities inherent in theories, the selection of the optimum model for the specific application is one of the more difficult tasks that design engineers have to fulfill. A comparative study among several candidate models help to examine the number of parameters, the degree of difficulty in determining these parameters, the predictive capabilities, the time of computing, and the implementation into a finite element code. For the monotonic and cyclic behavior of IN738LC, a nickel base superalloy used for turbine blades, and vanes, constitutive equations have been developed by Chaboche and Slavik and Schitoglu using united viscoplastic models. The Chaboche model assumes the existence of a yield criterion, which separates purely elastic from inelastic deformation. In comparison, no conventional yield criterion is used in the Slavik Schitoglu model and consequently, this approach allows for the possible existence of elastic and inelastic deformations at all stages of loading. Although they differ in their initial assumptions, these two models have already proved their high potential to describe the inelastic uniaxial behavior at high temperature of several nickel base superalloys as stated by E.Fleury and J.S.Ha<sup>[13]</sup>.

Critical components of GT such as blades and vanes are subjected to transient loading resulting from frequent startup, shutdown, and loading changes induced by daily and seasonal variations in the demand for electricity. Repetitions of these operations and the steady state gradients generally associated with cooling systems are typically of thermal fatigue loading conditions that are characterized by crack initiation and propagation, eventually followed by failure of the components. Since temperature gradients can not be eliminated, operating conditions should be fully understood and simulated with accurate modeling techniques. A simple form of thermal and technical testing called thermal mechanical fatigue testing, is developed in the 1970s to estimate in laboratory the loading conditions experienced by turbine blades and vanes. Thermomechanical fatigue testing offers several advantages. It can be conducted with a wide range of strain-temperature histories. It can be applied for material selection, and can be used to evaluate the capability of life prediction models. Life prediction models for non-isothermal conditions are classified into conventional engineering models and physically based models.

Conventional engineering models are based on the extension of models proposed for isothermal fatigue conditions. The shortcomings and limitations of these models have already been demonstrated. In comparison physically based life prediction models are considered to be promising tools for accurate predictions under non-isothermal loading conditions. In GTs, coatings are currently applied to blades and vanes not only to protect the underlying base metal against erosion, oxidation, and corrosion, but also to act as thermal insulation. However, it has been demonstrated that coatings can also alter the fatigue and creep resistance of substrate materials, as a result of the coating deposition process or post coating heat treatment<sup>[14]</sup>. A new process referred to TMF/TS-SRP has been developed to predict thermomechanical fatigue life of high temperature aerospace engine alloy. This is based on the total strain version of the method of strain range partitioning, the bi-thermal testing technique for characterizing TMF behavior, and advanced viscoplastic constitutive models. Predicted lives are in agreement with experimental lives to within a factor of approximately two<sup>[15]</sup>. The high temperature, low cycle, thermal and mechanical fatigue behavior has been investigated for high strength oxidation resistant superalloys used in aerospace propulsion systems. Advanced thermal life prediction methods have been based on strain controlled thermo-mechanical and load controlled, strain limited, bi-thermal fatigue tests<sup>[16]</sup>.

The cyclic life of IN738LC a widely used nickel based superalloy for blades in stationary gas turbines has been investigated under thermo-mechanical fatigue loading conditions using a temperature variation range of 1023-1233K with a suitable temperature variation rate. Simple thermo-mechanical cracks with linear sequence corresponding to in-phase (IP) and out-of-phase (OP) tests have been performed. Both the IP and OP tests have been carried out at different constant mechanical strain ranges between 0.8-2% and at a constant mechanical strain rate of 10.5/sec. Thermo-mechanical fatigue lives under both test conditions have been compared with each other and with those of isothermal LCF tests at a temperature of 1223K. The results show that the life under thermo-mechanical fatigue is strongly dependent on the nature of the test, i.e. stress controlled or strain controlled. A model is presented to develop predictions of thermo-mechanical fatigue crack initiation and estimate mode I growth of gas turbine hot section gas path superalloys. The model is based on a strain density fracture mechanism approach modified to account for thermal exposure and single crystal anisotropy. Thermo-mechanical fatigue crack initiation and small crack growth are modeled by employing an initial material defect size. Model capability is quantified by applying the model to two hot section gas path superalloys: uncoated MAR M509 and MCrAlY overlay coated PWA 1480. Thermo-mechanical fatigue model stresses have been obtained from nonlinear finite element analysis of thermo-mechanical fatigue specimen strain temperature history. Non-linear stress-strain behavior is predicted using unified viscoplastic constitutive models. Models of D.M.Nissley about thermomechanical fatigue life predictions are in good agreement with observed uniaxial thermomechanical fatigue specimen lives. Thermomechanical fatigue cracking depends upon coating thickness, single crystal anisotropy, crystal wave shape, dwell, and thermal exposure<sup>[17]</sup>.

The thermomechanical fatigue behavior of AMI nickel base superalloy single crystal has been studied using a cycle from 873-1373K. It is dependent on crystallographic orientation, which leads to different shapes of stress-strain hysteresis loops. The cyclic stress strain response is influenced by variation in Young's modulus, flow stress, and cyclic hardening with temperature for every crystallographic orientation. The thermomechanical fatigue life is controlled by crack growth. Depends on the mechanical strain range two main crack initiation mechanisms occur.

Oxidation induced cracking is the dominant mechanism in the lifetime of interest for turbine blade<sup>[18]</sup>.

During startup and steady state operation and shutdown gas turbine disks and blades made of superalloys are subjected to high-strain, low cycle fatigue due to the strain-temperature cycling, which leads to the failure of these critical components. The thermal-mechanical fatigue (TMF) test is employed to simulate the cyclic stress-strain behavior and damage process of these components in service. Investigations of F.Liu et.al. have shown that the thermal mechanical fatigue life of a real component is much shorter than that of isothermal fatigue (IF) at the maximum temperature and corresponding strain amplitude. The thermal-mechanical fatigue behavior of cast K 417 nickel based superalloys has been investigated under in-phase and out of phase loading in the temperature range from 673-1123K. The results reveal that the tendency to cyclic hardening under thermal-mechanical and isothermal fatigue is higher than that under static tensile testing at 1123K. Isothermal fatigue is observed to cause higher cyclic flow stress than TMF. At corresponding strain amplitude, the thermal-mechanical fatigue life has been lower than that of isothermal fatigue and the TMF life of out-of phase cycling is higher than that of in phase cycling. Scanning electron microscopic observations of fracture surfaces and longitudinal sections have revealed intergranular fracture under in phase TMF that lead to the decrease in fatigue life<sup>[19]</sup>.

### THERMAL FATIGUE

Cyclic strain controlled fatigue as opposed to cyclic stress controlled fatigue, occurs when the strain amplitude is held constant during cycling. Strain controlled cyclic loading is found in thermal cycling, where a component expands and contracts in response to fluctuation in the operating temperature or in reversed bending between fixed displacements. In a more general view, the localized plastic strain conditions result in strain controlled conditions near the roots of the notch due to the constraint effect of the larger surrounding mass of essentially elastically deformed material. The stresses do not necessarily need to come from mechanical stresses. Fatigue failure can be produced by fluctuating thermal stresses under conditions where no stresses are produced by mechanical causes. Thermal stresses result when the change in dimensions of a member as the result of a temperature change is prevented by some kind of constraint. If failure occurs by one application of thermal stress, the condition is called thermal shock. However if failure occur after repeated applications of thermal stress of a lower magnitude, it is called thermal fatigue. Thermal fatigues are frequently present in high temperature equipment (Allen, Forrest, and Ellison)<sup>[8]</sup>. Thermal shock and thermal fatigue test method involves electron beam heating of the surface of specimens using a thermal flux equal to that experienced during actual service operations. Two methods of electron beam radiation are described. In one method, the electron beam is swept across a narrow path with the specimen translated across the beam. In second method, the specimen remained stationary while the electron beam is repeatedly raster over a square shaped area. Similarity of thermal shock damage produced on rocket engine firing indicates that computer-controlled electron beam radiation can be used for determining thermal shock resistance of turbine blade material [19]. The mechanical processes involve in thermal fatigue degradation of cast-turbine blade material have been studied by an induction heating procedure coupled with an advanced alternating current potential drop system (ACPD). In particular, three temperature histories (cycle type) have been investigated using a double edge wedge specimen of cast IN-100 nickel base alloy. The respective stress-strain histories are determined from thermo-elastic-plastic finite element



analysis. The observed surface degradation depends on following model (i) scalloping and (ii) through thickness cracking of a uniform oxide layer. The degree of scalloping depends on the magnitude of compressive strain at the surface. Severe scalloping is observed after 3000 thermal cycles between peak strains of -0.48% at 1323K and +0.08% at 673K. More than 3000 cycles between peak strain of -0.24% at 1323K and 0.23% at 673K do not produce scalloping. The number of cycles to crack initiation is found to correlate with peak compression strain. Mechanisms of scallop initiation and growth involve cyclic oxidation cracking and cyclic ratcheting<sup>[20]</sup>.

Different location of microcracks in outer layers of CoCrAlY coating and inner layer of CoNiCrAlY coatings and separation of CoNiCrAlY coating through intermediate a-Cr layer have been reported in coated specimen after thermal cycling. The plastic intermediates layer between the base material (EP220, EP539) and CoCrAlY coating increases the life of alloy coating compound<sup>[21]</sup>.

In attempts of V.S.Bhattachar to explore the mechanism of thermomechanical fatigue of turbine blades the relationship between thermomechanical fatigue and matrix oxidation in a cyclic thermomechanical loaded IN 738 LC superalloy at 673-1173K in air has been investigated. SEM images indicate general as well as referential matrix oxidation of interdendritic and intergranular areas. It is suggested that the mechanical strain range influence the general matrix oxidation. The oxidation kinetics of a thermal fatigue behavior of polycrystalline nickel base superalloy-263 sheets has been studied using laboratory combustor system. Tests on 0.91 mm and 1.2 mm thick sheets square specimens (100'100 mm<sup>2</sup>) with a 14.85 mm diameter electro-discharge machined hole at the center at a maximum temperature is 1173K and a minimum temperature of 323K during a 2 minutes fatigue cycle have been conducted. The number of cycles to crack initiation has been determined. It is found that the change in sheet thickness does not significantly alter thermal fatigue life. Scanning electron micrographs reveals that out-of-phase non-isothermal fatigue (resulting from thermal stresses) assisted by grain boundary oxidation is the main mechanism of failure in these tests<sup>[22]</sup>.

### CORROSION FATIGUE

M.Yoshihara et.al. clarify the environmental effect of hot corrosion on the strength properties and fracture behavior of a nickel base superalloy subjected to different waveforms of loadings, fatigue, creep, and different kinds of combined creep-fatigue, by tests performed at 1073K on Inconel 751 specimens coated with a synthetic salt mixture composed of 90% Na<sub>2</sub>SO<sub>4</sub>-10% NaCl. The hot corrosion is found to induce serious degradation of the rupture life, depending on the loading conditions. In particular, the combined creep-fatigue tests result in a minimized rupture life in the corrosive environment, while monotonic creep cause the most prolonged life. A fatigue component in the loading is found to be responsible for the corrosion induced premature fracture, together with a creep component, although in air it plays only a minor role in the fracture behavior. The hot corrosion environment is also characterized by intergranular fracture in a brittle manner regardless of the loading conditions, which is directly caused by the stress-enhanced intergranular penetration of sulphides, oxides and or chlorides<sup>[23]</sup>.

The corrosion rate of the alloy IN-657 in the presence of a molten mixture of 60% V<sub>2</sub>O<sub>5</sub>-40% Na<sub>2</sub>SO<sub>4</sub> has been determined for the temperature range 950-1050K, in both oxidizing and inert atmospheres<sup>[24]</sup>.

**FATIGUE CRACK IN COMPONENTS**

Nickel base superalloys have been used with high reliability for blades and vane applications in gas turbines. Recently the application of directionally solidified and single crystal alloys has become common in advanced gas turbines, because of their superior creep and fatigue properties compared with conventionally cast polycrystalline materials. Effects of temperature, loading frequency, stress multiaxiality, environment, microstructure, and crystallographic orientation on the fatigue and creep strengths, have been studied on the directionally solidified single crystal superalloys. Current works mainly dealing with fatigue crack propagation at room temperature claim that an emphasis should be put on a study of small or short cracks of the order of microns. It is important to study small crack growth behavior the greater part of life is generally dominated by small crack initiation and propagation lives, and directly connected with the life prediction. Small cracks grow with the propagation rate significantly higher than that of accompanying physically long cracks (i.e. the difference in propagation rates between small and long cracks). The life prediction based on the traditional long crack results involves strong potential for non-conservative estimation. Small crack growth is notably affected by microstructures, such as grain boundary and strengthening precipitates, and by environment, than long cracks. The presence of small cracks is the cause of concern in creep-fatigue of high performance in nickel base superalloy, since the thickness of a gas turbine blade itself is in the order of millimeters. Nevertheless, there is very little, or inadequate information on the small crack growth process under creep-fatigue conditions. The effect of environment on the creep-fatigue small cracks is also a problem to be understood<sup>[25]</sup>. First it is essential to identify how at the microstructural scale, the instantaneous rate of fatigue crack growth is governed by the crack path selection mechanism. Secondly a statistical analysis of (i) crack arrest, (ii) instantaneous crack growth rates and (iii) and their dependence on linear elastic fracture mechanics parameters has to be done systematically. It is shown that all fatigue crack growth events occurring at the microstructural scale can be represented by a few statistical distributions. Thirdly, underlying slip band and dislocation mechanism of conventional fatigue in nickel base superalloys have to be understood<sup>[26]</sup>. High temperature 'dwell cracking' of the nickel base superalloy IN 718 is investigated by R.J.H. Wanhill as part of European project on military aircraft turbine discs. Dwell and fatigue crack growth tests under simple loading conditions indicate that dwell cracking would be unlikely to occur under actual flight loading and that standard fracture mechanics specimens may be inappropriate for predicting crack growth in discs. Flight by flight loading tests shows that dwell cracking is either absent or limited. Variables of investigations for fracture mechanics characterizations of dwell crack growth include peak loads and underloads on dwell crack growth; fatigue crack growth dwells in standard and engineering specimens, and crack growth under flight-by-flight loading, all at 873K<sup>[27]</sup>.

Crack growth tests have been performed on specimens with rectangular cross section of Inconel 718 at 823 and 960K in order to examine the low cycle fatigue behavior. Frequencies of 0.5 and 10 Hz are employed. Symmetric strain-controlled tests with a strain range of  $\Delta\epsilon = 1.5\%$  and load controlled zero tensile tests with a maximum load of 700 Mpa are performed. Fracture surfaces are examined to determine the fracture mode. At 960K the fracture surface is found to be intergranular at 0.5Hz and to be a mixture between inter and trans granular at 10 Hz. At 823K the fatigue specimens shown a mixed fracture mode at 0.5 Hz and a transgranular fracture mode at 50Hz. For the fatigued specimens showing an intergranular fracture mode, crack propagation rates as a function of stress intensity factor range proved to be time-dependent

and to be slightly higher than the pure creep crack growth rates. Experimentally observed crack growth rates have been used as input to a finite element simulation to determine the fraction of crack closure. The materials are described in terms of the visco-plastic constitutive equations developed by Bodner and Partom. The materials parameters are found by fitting simulations of the experimental data. Crack opening is found to take place almost immediately upon load reversal from a state of maximum compression<sup>[28]</sup>. Fracture crack growth rates (FCGR) are measured in a single crystal superalloy PWA 1480, in SEM specimens with different crystallographic orientations. Tests have been carried out at room temperature and at 1143K for two stress ratios:  $R = -1$ , and  $R = 0.1$ . A misorientation between the tensile axis and the<sup>[001]</sup> crystallographic direction has no effect on the FCGR regardless of test temperature or stress ratio. The stress ratio also has little effect on the FCGR. At room temperature, the fracture surfaces are highly crystallographic. The change in crack propagation path from a macroscopically mode I crack to large  $\{111\}$  facets results in higher growth rates. The observed fracture behavior can be interpreted on the basis of resolved shear stresses  $\{111\}$  planes ahead of the crack tip. At the elevated temperature, the fracture is completely non-crystallographic, and FCGRs are only mildly dependent on the direction of propagation as described by A. Diboine et.al.<sup>[29]</sup>.

Short-term fatigue growth of Waspalloy has been studied at room and elevated temperature. Tests are conducted at 292 and 773K reveal that the dominant mechanism of crack formation is slip band cracking. Crack formation is also associated with coarse carbide particles within the matrix. The dominant failure mechanism at 292 and 773K is one of mixed mode-I and -II fracture, with the mode-II shear displacement-giving rise to non-closure induced by surface roughness. Oxide and plasticity-induced non-closure process made only a minor contribution to the overall growth process. Short fatigue crack growth measured at  $R=0.1$  is faster at 773K than at 292K at an equivalent value of  $DK1$ . This is attributed to a change in slip character from highly planar to one involving increasing amounts of cross slip at 292 and 773K respectively<sup>[30]</sup>. The cyclic creep behavior of a nimonic 75 type alloy has been studied to understand intergranular fracture. Results show that at low stress amplitudes and high temperatures the fracture lives of cyclic creep and static creep are nearly equal. After normalization, all the data are found to obey approximately the linear cumulative law, showing that the change in fracture type does not alter the nature of creep-fatigue interaction<sup>[31]</sup>.

The optical crack monitoring system designed to examine the growth behavior of short/long fatigue cracks in Waspalloy at room and elevated temperature at stress ratio of 0.1 and -1 shows that the fatigue crack formation is associated with slip band cracking at both  $R=0.1$  and  $R=-1$ . The compressive part of the fatigue cycle at  $R= -1$  contributed to short crack growth at 292K and long crack growth at 773K<sup>[30]</sup>.

## PREDICTION OF FATIGUE LIFE ESTIMATION

Typical gas turbine and jet engine hot section components are subjected to severe environments along with variable thermal and mechanical load histories. Models for thermomechanical life predictions are based on creep-fatigue interactions exhibited by ductile metals, and do not explicitly contain environmental features. These models are viewed as parametric damage approaches, in which the environmental effect is assumed to be incorporated in the time dependence of the formulation<sup>[32]</sup>. Life predictions have been accounted from residual stress relaxation under cyclic loading. Finite element software is used for taking the cyclic plasticity

into account. The treatment of local plastic yield conditions can be made from elastic analysis. The J.Lu and L.F.Flavenot computed values of relaxed residual stress distributions are compared with experimental results obtained by X-ray diffraction measurements. The stabilized residual stress is calculated using a multiaxial fatigue criterion for life prediction<sup>[33]</sup>. Fatigue lifetime of R.Dauzer is given by the material's creep properties, if cyclic inelastic strain is steady state creep ( $r \sim 1$ ). The simple linear life fraction rule for creep damage (AC-rule) is used to calculate fatigue life. For  $r > 1$ , the AC rule overestimates fatigue lifetime. The deviation increases with increases of  $r$ . It is restricted to loading situations, where creep still has some influence. These conditions are characterized by  $r < 106$ <sup>[34]</sup>. The method for fatigue life prediction of high temperature polycrystalline materials under high rate fully reversed strain cycles (HRSC) is generalized using a continuous damage mechanics approach. It is assumed that creep deformation mechanism dominates during the creep portion of the fatigue cycle and that plasticity mechanism dominates during the plastic portion of the cycle. N.Matsuda et. al. have proposed that the frequency modified total strain energy parameter is useful for evaluating fatigue life and crack initiation life of a high strength superalloy under fatigue-creep interaction (FCI) conditions. Life prediction has been accounted of surface crack propagation behavior and initiation life in terms of grain size and number of cycles needed for surface crack length to grow to grain size<sup>[35]</sup>. Interaction of creep damage and fatigue damage has been developed for the high temperature superalloy 800H. The cavitation damage of internal grain boundaries during creep-fatigue experiments needs a nucleation stage and a growth stage. The latter exists for a slow deformation in tension and a first one in compression. Compression half cycle nucleates cavities. Shorter the time in compression more are the nuclei formed by interfacial decohesion of grain boundary carbides. The lifetime is determined by fatigue crack propagation, whose rate is controlled by (i) fast athermal deformation, (ii) creep deformation in tension and (iii) interaction with cavities<sup>[36]</sup>. Creep-fatigue life prediction under conditions of tension tensile stresses adopts the linear cumulative damage rule. However, a new method is advanced, namely, numerical computational approach of strain energy partitioning (SEP)<sup>[37]</sup>. J.Byrne et.al. illustrate that no matter how carefully manufacturing processes are controlled defects can still be present in materials going into service and surface damage of some form may inevitable when components and structures are put into application. Accordingly the damage tolerance approach may be used to monitor conditions and extend the life of components. The definition of damage tolerance is the ability of the structure or component to resist failure in the presence of flaw cracks or other damage for a specified period of usage. This method relies on the use of fracture mechanics to predict the behavior of cracks growing from origins with size fixed by material process control or non-destructive inspection. The gas turbine aeroengine disc is one of the most safety critical components in industrial use. If sub-surface defects are detected in a disc the whole batch may be scrapped, because of lack of understanding of their fatigue and fracture behavior which can be strongly affected by defects. Subsurface defects, in forged nickel based alloy discs are present due to chemical heterogeneity. When the disc surface has been shot peened and is under residual compressive stress, such subsurface defects may grow by fatigue or fatigue-creep at operating temperatures before the initiation of surface cracks. The size, shape, orientation, and distance below the surface will vary, influencing their fatigue crack growth (FCG) behavior and the cycle life ( $N_f$ )<sup>[38]</sup>. The initial hypothesis is that for given stress/strain intensity level, above the threshold for fatigue crack growth, defects would crack during the first loading cycle and thereafter the fatigue cyclic life ( $N_f$ ) would be entirely made up of crack propagation life. This could be characterized and modeled using fracture mechanics.

Conventional elevated temperature creep-fatigue life prediction techniques often assumes that the same deformation mechanism is operative over a range of extrinsic conditions, as for example strain levels, frequencies, and dwell times. Additionally, time dependent changes in intrinsic materials characteristics, as for example grain size and carbide distribution are often ignored. For example, one approach, due to Coffin and Manson establishes an empirical relationship between the plastic strain range and the fatigue life (cycles to failure). Coffin-Manson approach tends to yield non-conservative estimates of fatigue life when used under conditions, as for example at higher temperature or longer exposure times where time dependent phenomenon becomes increasingly important. Some improvement in predictive capability is possible through the introduction of a frequency term that is intended to account for time dependent effects. Alternative linear life fraction approach, adopted in ASME section IIIB and P.V.code case N-47, assumes that fatigue and creep damage phenomenon can be separated into cyclic and time-dependent components, and that those can then be linearly summed. Typically a total allowable damage of one is possible only when failure is ascribed to either pure creep or fatigue damage. When creep and fatigue interact the damage value falls below one, the exact design value is then defined from experimental data for each material under specified extrinsic conditions.

Oestergren recognized that mean stress effects has to be included in any successful high temperature life prediction approach. These mean stress effects arise from time dependent relaxation. This approach assumes the damage measure to be the net tensile hysteresis energy corresponding to the area in the hysteresis loop between the mean stress and ultimate stress. The physical measure is related to be the energy associated with crack propagation. This relation can again be modified to include time-dependent damage by introduction of a frequency term. While meeting various degrees of success, there are several limitations associated with the above mentioned life prediction methods. For example, the Coffin-Manson does not differentiate between loading cycles with or without hold times or between tension and compression strain rates as long as the frequencies and strain ranges are the same. Similarly, the linear life fraction methodology considers both tensile and compression hold times to be equally damaging not taking into account possible healing effects of the compressive cycle.

### NEURAL NETWORK APPROACH

Vasisht Venkatesh and H.J.Rack have produced a possible alternative approach entails artificial neural network (ANN), which has emerged as a powerful problem solving tool in signal processing, non-destructive testing, process control, corrosion life prediction, and material science. The architecture of an ANN is based on the human nervous systems that receive and process information. Each processing element (PE) receives input signals, from the environment or from other PRs and processes the weighted, sum of all the inputs through a threshold function.

An extensively used network is the back-propagation (BP) network, which consists of three or more layers of interconnected PEs. The first layer is the input layer, which consists of all the input factors. Information from the input layer is then passed through one or more hidden layers following which the output is computed in the final layer. In a BP network the knowledge, that is the relationship between input and output factors, is stored as the interconnected strength (i.e. the weights) between processing elements. In order for the network to be able to learn the relationship between input and output factors a training set consisting of known input and corresponding output sets is compiled. For each input in the training set the network computes

an output, the error between the computed and actual output is then calculated. Next error function is minimized using the gradient descent appraisal. These steps are repeated for all the training patterns until an acceptable error between the calculated and observed output, or a preset number of iterations, both of which are defined by the user prior to training, is achieved. Successful application of networks does however require that model inputs (based on physical process) network architecture (number of hidden arrows and layers), the learning rate, momentum term and the number of iterations be adjusted to develop an accurate BP model. Optimization of the back propagation network performance can be accomplished using a statistical design approach. Improved network performance can be judged by minimizing the standard deviation. A linear correlation between predicted and experimental values in the training set can be used as an indicator of the level of network training. The higher is the correlation value; the better is the training. Over training of the network can lead to high correlation values and poor network memorizing the training sets. Recently, increased interest has been shown in utilizing INCONEL 690 for nuclear waste nitrification components operating at temperatures above 0.75 Tm where INCONEL 690 is metallurgical unstable, both carbide dissolution and extensive grain growth having been observed. These latter studies have also shown that such microstructure instabilities have a major impact on the deformation mechanisms observed during constant stress loading, a transition in primary deformation mechanism from matrix controlled dislocation motion to grain boundary sliding and migration being observed. This material is therefore an excellent candidate for examining the potential applicability and limitations of the neural network approach for creep-fatigue life prediction. The objective of this research is aimed at examining this new method and comparing its predictive capability with those of the Coffin-Manson, linear life fraction and the hysteresis energy techniques for the design of components operating at high temperatures (0.7-0.8 Tm)<sup>[39]</sup>.

## JET ENGINE, LINERS, AND PERFORMANCE OF SUPERALLOYS

### *Jet engine*

The jet engine a very complex but operationally simple device as shown in Fig. 1 (a GE 90-115B engine) consists of a stationary, hour-glass-shaped, cylindrical case on which all of the vanes (nozzles) and the combustion chamber (combustor) are attached, and a rotating mandrel on which a series of disks (rotors, wheels) are mounted. The efficiency and performance of the jet engine are strongly dependent on the highest temperature in the engine, the inlet temperature of the HPT, and it is the high-temperature capability of the parts that is critical. Higher operating temperatures must be realized to achieve higher thrust. Engines must be made significantly lighter without loss of thrust to achieve higher efficiency. In both cases, it is obvious that completely new families of materials must be developed with higher melting points along with greater intrinsic strength<sup>[40]</sup>.

### *Liner of combustion chamber*

The liner of can type chamber is perforated inner liner with housings and encasings. The larger section of chamber body encases the liner at the exit end; the smaller chamber-cover encases the front or inlet end of the liner. Each can is a separate burner and flame is located at the chamber liners. Liners of can type combustor have perforations of various sizes and shapes, each hole having a specific purpose and effect on flame propagation in the liner. Holes, louvers, and slots into two main streams, (i) primary, and (ii) secondary air, device air entering the

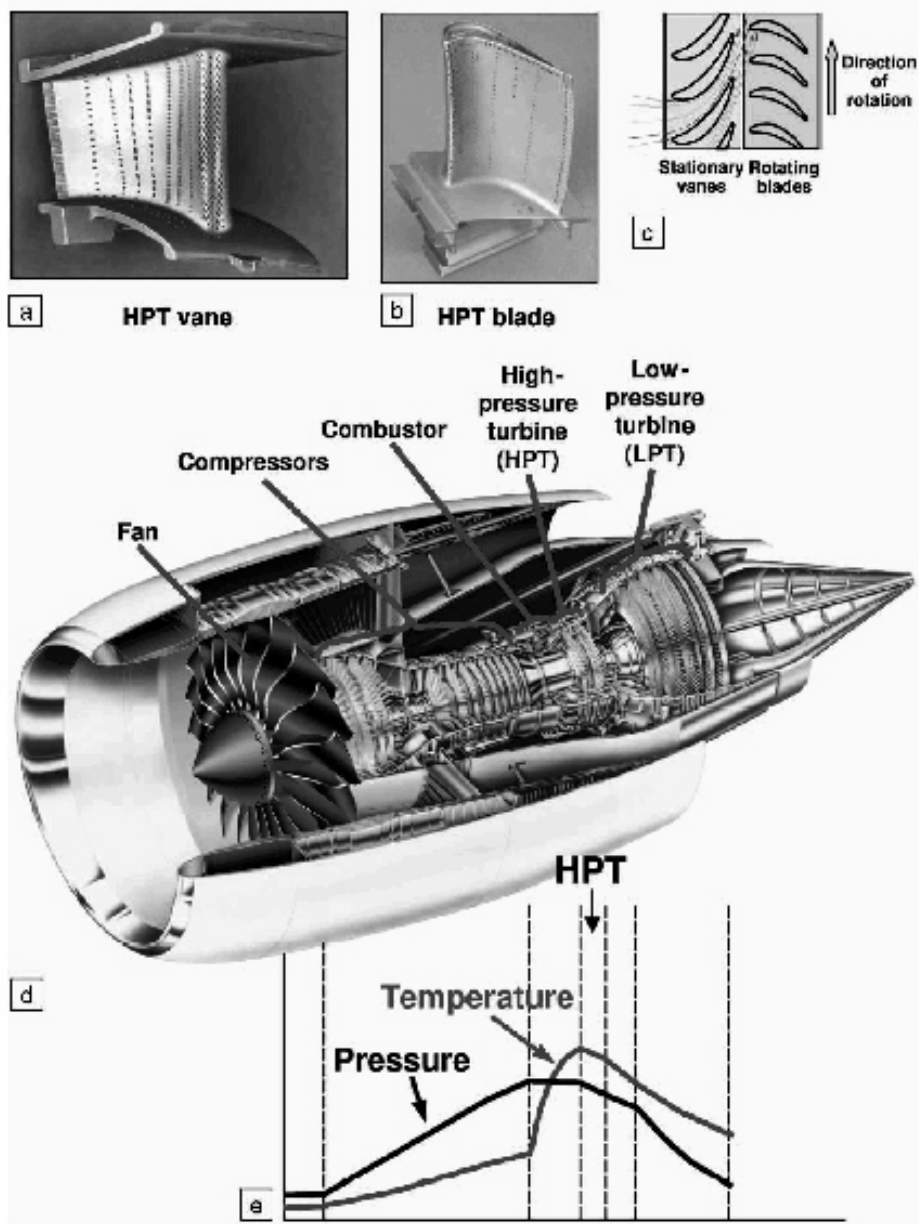


Fig. 1 : (a) and (b) photographs of a high pressure turbine (HPT) vane and a HPT blade of a jet engine, (c) schematic arrangement of the stationary vanes relative to the rotating blades with the engine, (d) illustration of the GE90-115B jet engine, showing its various components, (e) pressure and temperature trends from the front to the back of the engine<sup>[40]</sup>.

combustion chamber. Primary (combustion) air is directed inside the liner at the front end where it mixes with the fuel and burns. Secondary (cooling) air passes between the outer casing and the liner and joins the combustion gases from about 2200K to near 1089K. Holes around fuel nozzle in the dome or inlet end of the can type combustor liner aid in atomization of the fuel. Louvers are also provided along the axial length of liners to direct a cooling layer of air along the inside wall of the liner. This layer of air also tends to control the flame pattern

by keeping it centered in the liner, preventing burning of the liner walls. Fig. 2 shows a single-shaft turboprop engine (Rolls-Rouce Dart). This illustrates use of a centrifugal compressor and can typr combustion chamber within years of 1953 and 1985<sup>[41]</sup>.

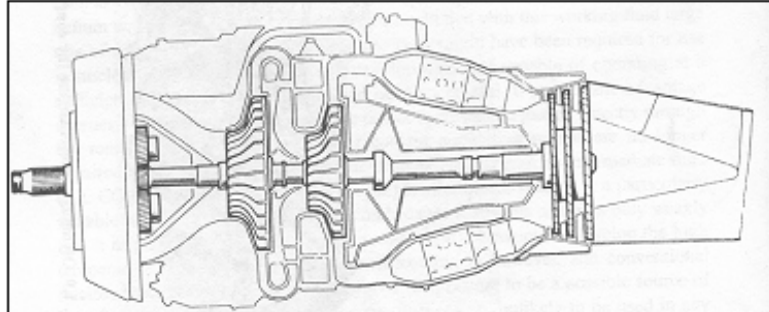


Fig. 2 : Single-shaft turboprop engine<sup>[41]</sup>.

Fig. 3(a) is a line diagram of aircraft sector double annular combustor in parallel staging. Fuel flow is adjusted to both annuli, so as to provide lean fuel/air ratios at high powers. Alternatively axially staged combustion is developed to result in a longer combustion than annular arrangement. The staggered inline arrangement reduces length penalty and has greater potential for emission reduction (Fig. 3(b))<sup>[40]</sup>. General Electric has approached multiple combustor for heavy industrial gas turbines. The design is based on modification of cans. The original can had a single burner, but a ring of six primary dual-fuel burners surrounding a single secondary dual-fuel burner has replaced this. The convergent-divergent section of primary zone and venturi of secondary zone respectively accelerates the flow and stabilize flame by recirculation (Fig. 3(c))<sup>[40]</sup>.

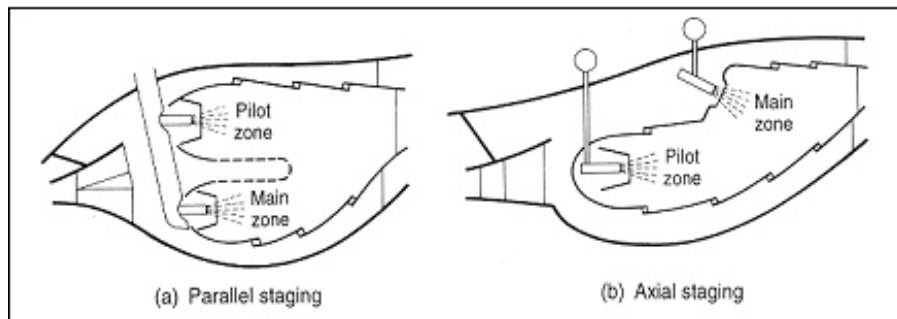


Fig. 3 (a) and (b) : Low-emission aero-engine combustors<sup>[41]</sup>.

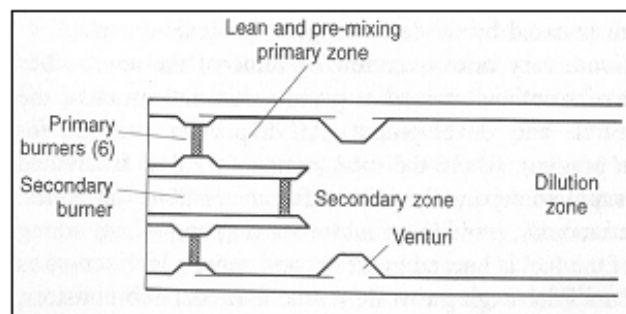


Fig. 3(c) : Can for General Electric low NOx combustor<sup>[41]</sup>.



Annular or basket type combustion chamber liner is an undivided circular shroud extending all the way around the outside of the turbine shaft housing. The chamber may be constrained of one or more baskets. If two or more chambers are used then one is placed outside the other in the same radial plane, hence the term double annular chamber. Its use permits building an engine of small diameter. Instead of individual combustion chambers, the compressed air is introduced into an annular space formed by a combustion chamber liner around the turbine shaft. Usually, enough space is left between the outer liner wall and the combustion chamber housing to permit the flow of cooling air from the compressor. Some axial compressor engines have a single annular combustion chamber. The liner of this type of burner consists of continuous circular, inner, and outer shrouds around the outside of the compressor drive shaft housing. Holes in the shrouds allow secondary cooling air to enter the center of the combustion chamber. Fuel is introduced through a series of nozzles at the upstream end of liner. Because of their proximity to the flames all types of burner liner are short-lived in comparison to other engine components; they require more frequent inspections and replacement.

Liners of can-annular type design of combustion chamber (Pratt and Whitney) contains a central bullet shaped perforated liner. The size and shape of holes are designed to admit the correct quality of air through holes and louvers of the can-annular chambers. This is almost identical with the flow through other types of burners. Special baffling is used to swirl the combustion airflow and to give it turbulence<sup>[42 - 44]</sup>. Alan S. Feitelberg et.al. show schematic of RQL-2 can-annular combustor (Fig. 4,<sup>[42]</sup>) with experimental test stand.

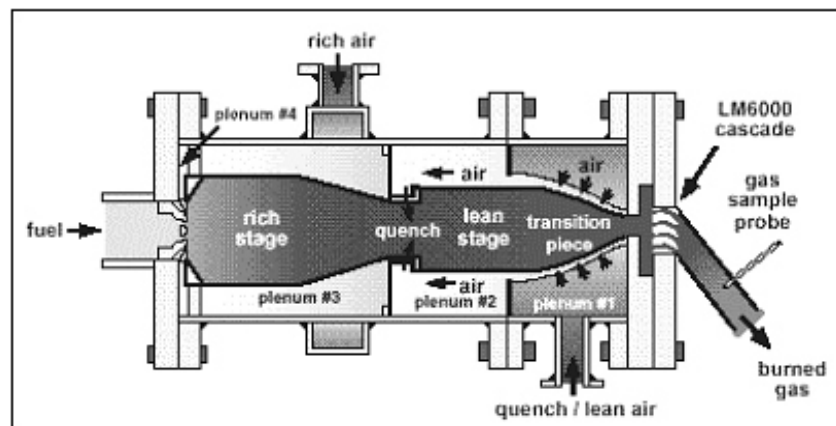


Fig. 4 : RQL 2 combustor and test stand<sup>[42]</sup>.

#### High temperature performance of superalloys

Heat-treated superalloys enter service in a metastable condition, therefore change in microstructure and mechanical properties occur during exposure to service temperature. R.Sivakumar and B.L.Mordike describe these changes in several forms. At 873-1173K, some alloys develop topological close packed phase (TCP), such as s, m, and Laves. These phases are hard and brittle and often occur as platelets or needles so that their formation is often associated with loss in ductility and impact strength. Furthermore, since they grow by absorbing strengthening elements from the matrix, creep and stress rupture properties may be affected adversely. Some early alloys are prone to extensive TCP formation that has resulted in almost total loss of ductility during service operation. However, the use of electron vacancy theory to

predict the susceptibility of alloy compositions to form TCP phases is now well established and has enabled TCP formation to be controlled to acceptable levels in current commercial alloys. Alloys containing a significant carbon level (0.02-0.1%) show a significant decrease in room temperature ductility on exposure as a result of precipitation of secondary carbides. The low residual ductility of Hastelloy-X and Haynes-188 has been ascribed to precipitation of secondary carbides in conjunction with formation of s and m phases in Hastelloy-X and Laves phases in Haynes-188. The ductility may be completely restricted by a solution treatment. More recent alloys that have been designed to be free from TCP formation show far less degradation. For example Haynes-230 retains 70% or more of its original ductility. Exposure at temperatures above 1173K-cause solution and/or precipitation of secondary phases and changes associated with oxidation process. Oxidation process may take the form of surface fissuring, oxide spalling, with a consequent reduction in section thickness; and subsurface compositional and microstructural changes such as chromium depletion, carburisation, internal oxidation and formation of intermetallics. All of which may involve considerable migration

Table 1 : Main characteristics of some sheet alloys (Fig. 5)<sup>[45]</sup>.

Alloy	Type	Main attributes	Limitations
Nimonic 75	Solid solution	Readily fabricated, simple heat treatment	Low strength especially above 1073K, susceptible to oxide scaling
Hastelloy X	Solid solution and carbide strengthened	Adequate fabricability, useful level of strength to 1073K, more tolerant of salt/carbon attack than most nickel-base alloys	Strength limited above 1073K susceptible to oxide fissuring at hot spots
Nimonic 263	Solid solution and precipitation strengthened with	Excellent strength to about 1093K, readily fabricated	Overages rapidly above 1093K, intergranular oxidation becomes excessive above 1223K.
Haynes 188	Solid solution and precipitation strengthened, contains lanthanum to improve oxidation resistance	The strongest conventional sheet alloy at temperatures above 1073K, acceptable fabricability	Susceptible to oxide spalling at temperatures above 1323K, high forming loads, high annealing temperature
Nimonic 86	Solid solution, contains cerium to improve oxidation resistance	Good all-round balance of properties, especially oxidation resistance, readily fabricated	Strength limited
Inconel 617	Solid solution and carbide strengthened	Excellent high-temperature strength of the same order as that of Haynes 188, acceptable fabricability	Susceptible to oxide fissuring
Haynes 230	Solid solution and carbide strengthened	Excellent oxidation resistance, good strength above 1073K.	Currently being evaluated

and segregation of the elemental constituents. Subsurface changes are especially important with thin section material since at temperature of the order of 1323K the changes may eventually penetrate the full thickness of the material. Deterioration is associated with pronounced growth of carbides at grain boundaries and solution of the fine matrix carbides. Grain boundary coarsening is more extensive and more continuous in Inconel-617 than in other alloys so that failures become increasingly intergranular as the soaking duration is increased. Oxidation effects cause the deterioration of Hastelloy-X, Haynes-188, and Inconel-617 in the later stages of soaking. Inconel-617 develops extensive oxide fissuring. Haynes-188 is prone to oxide spalling with a consequent reduction in section thickness, while Hastelloy-X is susceptible to both fissuring and oxide spalling. Consequently on the basis of microstructure stability and oxidation resistance at 1323K, Haynes-230, and Nimonic-86 are superior to Haynes-188, Hastelloy-X, and Inconel-617. Figure 5 shows the comparative trend of different sheet metal properties that are used in combustor manufacture. The high temperature behaviors are tabulated (Table 1) by B.Hicks<sup>[45]</sup>.

Corrosion and oxidation are results of electrical and chemical reactions with other materials. The hot exhaust gas stream encountered in the engine speeds up this reaction. If the oxide coating is porous or has a coefficient of expansion different from that of the base metal, the base metal will be continually exposed to the oxidizing atmosphere. One solution to oxidation at elevated temperature is ceramic coatings. Ceramic coated after burner liners and combustion chambers are in use today. The ceramic coating has two basic functions. (1) Sealing the base metal surface against corrosion, (2) Insulating the base metal against high temperature. These coatings are not without disadvantages, they are more susceptible to thermal shock<sup>[46, 47]</sup>, they must have the same coefficient of expansion as the base metal, they are brittle, and they have low tensile strength that restricts their use in the engine. Sever engine failures have been attributed to thermal shock on the turbine disc. Ceramic coating in particular is vulnerable to this form of stress. Improved fuel controls, starting techniques, and engine design have lessened the problem<sup>[47]</sup>.

## REFERENCES

1. Sawarin Y., Astafjev V., Maclakov V. and Semenychev V., (1988) The structural life prediction under creep or high-cycle fatigue conditions, Fracture Analysis-Theory and practice, Vol. 1 [Proc.Conf.], Budapest, Hungary, 19-24 Sept. 1988, Eng. Mater. Advisory Services Ltd., 339 Halesowen Rd., Cradley Health, Warley, West Midlands B 646 PH, UK, (Met. A, 9101-72-0013), pp. 344.
2. Shyam A., Padula II S.A., Marras S.I., and Milligan W.W., (2002), Metall. and Mater. Trans. A, 33A, pp. 1949.
3. Zhang J.H., Xu Y.B., Wang X.G., and Hu Z.Q., (1995), Scripta Metall. Mater., 32(12), pp. 2093.
4. Padula II S.A., Shyam A., Ritchie R.O., and Milligan W.W., (1999), Int. J. of Fatigue, 21(7), pp. 725-731.
5. Kussmaul K., Maila K., and Bothe K., (1995), Mater. Wiss. Technol., 26(5), pp. 241-250.
6. Gieseke B., and Sikka V. K., (1992), The effect of casting temperature on the fatigue properties of cast nickel aluminide alloys, 2nd Int. ASM Conf. On high temperature aluminides and intermetallics II [Proc.Conf.], SanDiago, California, USA, 16-19 Sept. 1991, Mater.Sci. Eng.A, A, Vol. 153, No. 1-2, Pp. 520-524, 30th May (1992).
7. Tong J., Dalby S., Byrne J., Henderson M.B., and Hardy M.C., (2001), Int. J. of Fatigue, 23, pp. 897-902.

8. Dieter George E., (1987), Mechanical Metallurgy, 3rd Ed., Book chapter, Chap. 12, and 13, pp. 375-470.
9. Li S.X., and Smith D. J., (1995), Fatigue Fracture Eng. Mater. Struct., 18(5), pp.631-643.
10. Martinez-Esnaola J. M., Martin-Meizoso A., Affeldt E. E., Bennett A. and Fuentes M., (1997), Fatigue and Fracture of Engineering Materials and Structures, 20(5), pp. 771-788.
11. Smith D. J., Shu-Xiu L., and Ellison G. E., (1992), Influence of orientation on the fatigue and creep behavior of a single crystal nickel base superalloys, Creep: Characterisation, Damage, and Life assessments [Proc. Conf.], Lake Buena Vista, Florida, USA, 18-21 May 1992, ASM Int., Materials Park, Ohio 44073-002, USA, pp. 603-608.
12. Matsubara M., Nitta A., and Kumabara K., (1991), J. Soc. Mater. Sci., Jpn., 40 (454), pp. 901-907.
13. Fleury E. and Ha J. S., (2001), Mater. Sci. and Technol., 17, pp. 1079-1086.
14. Fleury E. and Ha J. S., (2001), Thermomechanical fatigue behavior of nickel base superalloy IN 738 LC Part-2-Life time prediction, Mater. Sci. and Technol., 17, pp. 1087-1092.
15. Halford G. R., Saltsman J.F., Verrilli M.J., and Arya V.K. (1990) Application of thermal life prediction model to high temperature aerospace alloys B 1900 + Hf and Haynes 188, NASA Lewis Research Center, N 91-19473/8/XAB, Pp. 12.
16. Halford G. R., Verrilli M. J., Kalluri S., Ritzert F. J. and Holland F. A., Duckert R. E., (1991), Thermomechanical and bi-thermal fatigue behavior of cast B1900 + Hf and wrought Haynes 188, NASA Lewis Research Center, N91-20268/9/XAB, pp. 22.
17. Nissley D. M., (1995), AIAAJ, 33(6), pp. 1114-1120.
18. Mei Z., Krenn C. R., and Morris J. W. Jr., (1995), Metall. Mater. Trans.A, 26A (8), pp. 2063-2073.
19. Liu F., Ai S. H., Wang Y. C., Zhang H. and Wang Z. G., (2002), International Journal of fatigue, 24, pp. 841-846 ([www.elsevier.com/locate/ijfatigue](http://www.elsevier.com/locate/ijfatigue)).
20. Marchand N. J. and Dorner W., (1991), Mater. High Temp., 9(4), pp. 217-227.
21. Rybnikov A. I., Ugurtzov A. P., Tchizhik A. A. and Getzov L. B., (1991), Thermal fatigue resistance of gas turbine blades protective coatings TATF91: 3rd Int. Symp. On trends and new applications in thin films [Proc. Conf.], Strasbourg, France, 25-29 Nov.(1991), Vide. Couches Minces (Suppl. 259), pp. 138-140, Nov.-Dec..
22. Bhattachar V. S., (1995), Int. J. of Fatigue, 17 (6), pp. 407-413.
23. Yoshiba M., Miyagawa O. and Hamauaka T., (1990), Tokyo Metropolitan University, Boshoku Gijutsu (Corrs. Eng.), 39 (3), pp. 132-140, Mar..
24. Pardo A., Otero E., Hermaez J. and Perez F. J., (1992), Mater. Charact., 29(1), pp. 1-6.
25. Okazaki Masakazh and Yamazaki Yasuhiro, (1999), Int. J.of Fatigue, 21, pp. S79-S86.
26. Boyd-Lee A. D., (1999), Int. J. of Fatigue, 21, pp. 393-405.
27. Wanhill R. J. H., (2002), Int. J. of Fatigue, 24, pp. 545-555.
28. Anderson H., Persson C. and Hansson T., (2001), Int. J.of Fatigue, 23, pp. 817-827.
29. Diboine A., Paltier J. M. and Pelloux R. M., (1990), Fatigue crack propagation in a single crystal nickel base superalloys, Massachusetts Institute of Technology, High temperature fracture mechanisms and mechanics [Proc. Conf.], Dourdan, France, 13-15 Oct. (1987), Mech.Eng.Pub., P.O.Box 24, Northgate Avenue, Bury St Edmunds, Suffolk, IP326BW, UK, pp. 421-446.

## FATIGUE IN GAS TURBINE COMPONENTS

30. Hearly J. C., Bcevers C. J. and Grabowski L., (1992), *Fatigue Frac. Eng. Mater. Struct.*, 15(3), pp. 309-321.
31. Wang D. N., Wang X. and Kong Q. P., (1991), *Academia Sinica. Mater. Sci. Eng. A*, A142(2), pp. 157-161.
32. McDowell D. L., Autolovich S. D. and Oahmke R. L. T., (1992), *Nucl. Eng. Des.*, 133 (3), pp. 383-399.
33. Lu J. and Flavenot L. F., (1988), Prediction of the fatigue life taking into account residual stress relaxation under cyclic loading, CETIM, Failure Analysis Theory and Practice, Vol. 1 [Proc. Conf.], Budhapest, hungary, 19-24th Sept. (1988), Engg. Materials Advisory Services Ltd., 339 Halesowen Rd., Cradly Health, Warley, West Midlands B646PH, UK.
34. Dauter R., (1992), The influence of creep on the fatigue life of nickel base superalloys, Creep, Characterisation, Damage and Life assessment [Proc.Conf.], Lake Buona Vista, Florida, USA, 18-21 May (1992), ASM Int., Mater. Park, Ohio 44073-0002, USA, (Met. A, 9211-72-0495), pp. 359-368.
35. Matsuda N., Umezawa S. and Hitachi J., (1990), *J. Soc. Mater. Sci.*, 39(439), pp. 419-424.
36. Mu Z. and Gerold V., (1991), *Z. Metallkd.*, 82(8), pp. 633-639.
37. Su H., and He J., (1989), *Mater. Mech. Eng. (China)*, 13 (4), pp. 30-32.
38. Byrne J., Kan N. Y. K., Hussey J. W. and Harrison G. F. J. of *Fatigue*, (1999), 21, pp. 195-206.
39. Venkatesh Vasisht and Rack H. J., (1999), *Int. J. of Fatigue*, 21, pp. 225-234.
40. Zhao J. C. and Westbrook J. H., (2003), *MRS Bulletin*, pp. 522-530. ([www.mrs.org/publications/bulletin](http://www.mrs.org/publications/bulletin)).
41. Cohen H., Rogers G. F. C. and Saravanamuttoo H. I. H., (1996), *Gas turbine theory*, 4th edition, Book chapter, pp. 233-267.
42. Feitelberg Alan S., Jackson Melvin R., Lacey Michael A., Manning Kenneth S. and Ritter Ann M. Design and performance of a low Btu fuel rich-quench-lean gas turbine combustor, GE corporate Research and Development, PO. Box 8, Schenectady, NY 12301, [http://www.netl.doe.gov/publications/proceedings/96/96ps/ps\\_pdf/96ps1\\_7.pdf](http://www.netl.doe.gov/publications/proceedings/96/96ps/ps_pdf/96ps1_7.pdf).
43. Meetham G. W., (1981), The development of gas turbine materials, Book chapter, pp.1-30, pp. 259-290.
44. Sheffler K. D. and Gupta D. K., (1988), Current status and future trends in turbine applications of thermal barrier coatings, ASME Paper 88-GT-286.
45. Hics B., (1987), High temperature sheet materials for gas turbine applications, *Mater. Sci and Technol.*, Vol. 3(9), pp. 772-781.
46. Bede W., (1997), Reliable TBC's for the industrial gas turbine design. 1997 TMS Annual Meeting: Materials coatings and processes for improved reliability of high temperature components: Session IV: life prediction, NDE, and repairs, Cincinnati, OH-45215.
47. Tolpygo V. K., Clarke D. R. and Murphy K. S., (2001), *Metall. and Mater. Trans.A*, 32A, pp. 1467-1478.